

Critical behavior at edge singularities in one dimensional spin models

D. Dalmazi* and F. L. Sá†

UNESP - Campus de Guaratinguetá - DFQ

Av. Dr. Ariberto P. da Cunha, 333

CEP 12516-410 - Guaratinguetá - SP - Brazil.

October 25, 2018

Abstract

In ferromagnetic spin models above the critical temperature ($T > T_{cr}$) the partition function zeros accumulate at complex values of the magnetic field (H_E) with a universal behavior for the density of zeros $\rho(H) \sim |H - H_E|^\sigma$. The critical exponent σ is believed to be universal at each space dimension and it is related to the magnetic scaling exponent y_h via $\sigma = (d - y_h)/y_h$. In two dimensions we have $y_h = 12/5$ ($\sigma = -1/6$) while $y_h = 2$ ($\sigma = -1/2$) in $d = 1$. For the one dimensional Blume-Capel and Blume-Emery-Griffiths models we show here, for different temperatures, that a new value $y_h = 3$ ($\sigma = -2/3$) can emerge if we have a triple degeneracy of the transfer matrix eigenvalues.

*dalmazi@feg.unesp.br

†ferlopessa@yahoo.com.br

1 Introduction

In [1] C. N. Yang and T.D. Lee have initiated a method to study phase transitions based on partition function zeros. Since then, several applications have appeared in equilibrium and more recently in non-equilibrium statistical mechanics, see [2] for a review and references. It is expected that with the increase of computer power new applications will appear specially where analytic methods can hardly be used. In many statistical models the so called Yang-Lee zeros (YLZ) lie on arcs on the complex u -plane, $u = \exp(-\beta H)$, where H is an external magnetic field and $\beta = 1/K_B T$. The zeros at endpoints of the arcs tend to pinch the positive real axis $\Re(u) > 0$ at the critical value of the magnetic field for $T \leq T_{cr}$ while for $T > T_{cr}$ they accumulate at complex values $u_E = \exp(-\beta H_E)$ which are called Yang-Lee edge singularities (YLES). The linear density of zeros has a universal power like divergence $\rho(u) \sim |u - u_E|^\sigma$ in the neighborhood of the YLES. The critical properties of the YLES are described by a non-unitary $\nu\varphi^3$ field theory [3] which corresponds in two dimensions [4] to a $(p, q) = (2, 1)$ non-unitary conformal minimal model leading to the prediction $\sigma = -1/6$. This is in agreement with numerical results for the ferromagnetic Ising model, see e.g. [5, 6], and experimental magnetization data [7]. Even in the anti-ferromagnetic Ising model where $u_E \in \mathbb{R}_-$ numerical results [8] also lead to $\sigma = -1/6$. Analogously, for the ferromagnetic and anti-ferromagnetic $S = 1/2$ Ising model in $d = 1$ one derives exactly $\sigma = -1/2$. In the ferromagnetic case, the value $\sigma = -1/2$ has been found in other $d = 1$ models like the n -vector chain [9] and the q -state Potts model with $q > 1$ and $0 \leq q < 1$ [10]. Furthermore, in [11], by assuming that the transfer matrix eigenvalues are real in the gap of zeros and that the magnetic field is pure imaginary, one obtains $\sigma = -1/2$ for the $S = 1, 3/2$ Ising model and also for the Blume-Emery-Griffiths (BEG) model investigated here. The same assumptions of [11] have been made in the proof of $\sigma = -1/2$ given in [12, 9]. More recently [13] another proof which holds without those assumptions has appeared in the Blume-Capel model. We show here that the latter proof contains also some hypotheses which are not satisfied in part of the parameter space of the BEG model where a new critical behavior appears.

2 General setup and analytic results

Our starting point is the couple of finite size scaling (FSS) relations, see [14, 15], :

$$u_1(L) - u_1(\infty) = \frac{C_1}{L^{y_h}} + \dots \quad (1)$$

$$\rho(L) = C_2 L^{y_h-d} + \dots \quad (2)$$

where C_1, C_2 are constants, independent of the size of the lattice L . The Yang-Lee zero $u_1(L)$ is the closest zero to the edge singularity $u_E = u_1(\infty)$. The density of zeros $\rho(L)$ is calculated at $u = u_1(L)$. In practice we use

$$\rho(L) = \frac{1}{N|u_1(L) - u_2(L)|} \quad , \quad (3)$$

where $u_2(L)$ is the second closest zero to u_E and N is the total number of spins ($N = L^d$). The dots in (1),(2) stand for corrections to scaling. Our analytic method consists of deriving y_h from an expansion for large number of spins similar to (1) obtained directly from the transfer matrix solution. We also calculate the YLZ numerically for finite number of spins and check the validity of (1),(2) which furnish numerical estimates for y_h .

The partition function for the BEG model is given by [16]

$$Z_N = \sum_{\{S_i\}} \exp \beta \left\{ J \sum_{\langle ij \rangle} S_i S_j + K \sum_{\langle ij \rangle} S_i^2 S_j^2 + \sum_{i=1}^N [H S_i + \Delta (1 - S_i^2)] \right\} \quad , \quad (4)$$

where $S_i = 0, \pm 1$ and the sum $\sum_{\langle ij \rangle}$ is over nearest-neighbor sites. We assume ferromagnetic Ising coupling $J > 0$ but K, Δ can have any sign. All the couplings J, K, Δ are real while the magnetic field H may be complex. The temperature is defined with respect to the ferromagnetic coupling via the compact parameter $c \equiv \exp(-\beta J)$, where $0 \leq T < \infty$ corresponds to $0 \leq c \leq 1$. In $d = 1$, using periodic boundary conditions, $S_i = S_{i+N}$, the model can be easily solved via transfer matrix :

$$Z_N = c^{-N} [\lambda_1^N + \lambda_2^N + \lambda_3^N] \quad , \quad (5)$$

where the eigenvalues $\lambda_1, \lambda_2, \lambda_3$ are the solutions of the cubic equation

$$\lambda^3 - a_2 \lambda^2 + a_1 \lambda - a_0 = 0 \quad , \quad (6)$$

with coefficients

$$\begin{aligned} a_0 &= b \tilde{x} (1 - c^2) [b(1 + c^2) - 2c] \\ a_1 &= b^2 (1 - c^4) + A \tilde{x} (b - c) \\ a_2 &= \tilde{x} + A b \end{aligned} \quad (7)$$

We have defined for convenience

$$b = \exp(\beta K) \quad , \quad x = \exp(\beta \Delta) \quad , \quad \tilde{x} = xc = \exp \beta(\Delta - J) \quad (8)$$

$$A = u + 1/u = 2 \cosh(\beta H) \quad (9)$$

The quantity $u = \exp(-\beta H)$ plays the role of fugacity in a lattice gas [1]. The partition function Z_N is proportional to a polynomial of degree $2N$ in the fugacity. Therefore, all relevant information about Z_N is contained in its zeros $Z_N(u_k) = 0$, $k = 1, \dots, 2N$. Due to \mathbb{Z}_2 symmetry, $Z_N(u) = Z_N(1/u)$, half of the zeros are the inverse of the other half. The exact position of the YLZ can hardly be found even in one dimension. In the thermodynamic limit the partition function will vanish whenever two or more eigenvalues share the largest absolute value, see [17, 18, 10]. For large finite number of spins the same conditions are still useful, see e.g. [19], for locating the YLZ. Thus, following [13], let us assume that there exists a function $A(\varphi) = u(\varphi) + u^{-1}(\varphi)$ such that when we plug it back in (6) we have:

$$\lambda_2 = e^{i\varphi} \lambda_1 \quad (10)$$

$$|\lambda_2| = |\lambda_1| > |\lambda_3| \quad (11)$$

Therefore, for a large number of spins we can neglect the contribution of λ_3 and write $Z_N \approx |\lambda_1|^N (1 + e^{iN\varphi})$. The $2N$ YLZ are found from

$$u^\pm(\varphi_k) = \frac{1}{2} \left[A(\varphi_k) \pm \sqrt{A(\varphi_k)^2 - 4} \right] \quad , \quad (12)$$

with $\varphi_k = (2k - 1)\frac{\pi}{N}$, $k = 1, 2, \dots, N$. In order to find $A(\varphi)$ we start from the relations $a_0 = \lambda_1 \lambda_2 \lambda_3$, $a_1 = \lambda_1 \lambda_2 + \lambda_1 \lambda_3 + \lambda_2 \lambda_3$, $a_2 = \lambda_1 + \lambda_2 + \lambda_3$. Implementing the condition (10) and eliminating λ_3 we obtain:

$$a_1 = \lambda_1 a_2 (1 + e^{i\varphi}) - \lambda_1^2 (1 + e^{i\varphi} + e^{i2\varphi}) \quad (13)$$

$$a_0 = \lambda_1^2 a_2 e^{i\varphi} - \lambda_1^3 (e^{i\varphi} + e^{i2\varphi}) \quad (14)$$

Manipulating (13) and (14) we further eliminate λ_1 and find an equation for $A(\varphi)$:

$$a_0^2 (1 + 2 \cos \varphi)^3 + 4 \cos^2 \frac{\varphi}{2} (a_1^3 + a_0 a_2^3) - a_1^2 a_2^2 - 2 (1 + 2 \cos \varphi) (2 + \cos \varphi) a_0 a_1 a_2 = 0 \quad (15)$$

which is the same expression obtained in [13] for the Blume-Capel model ($b = 1$). At this point, in principle, the Yang-Lee zeros are determined by (15), once we check (11). After taking the continuum limit in the corresponding solution $u(\varphi_k)$ one could derive the density of zeros and obtain the exponent σ . However, in practice, the expression (15) is a fourth degree polynomial equation for $A(\varphi)$ whose solutions are cumbersome in general. It is not feasible to substitute them in the solutions of the cubic equation (6), which are a bit complicated too, and then check the condition (11) for arbitrary values of the parameters b, c, x .

Fortunately, in order to compute the exponent σ or y_h we only need to study the vicinity of the YLES. The YLES is located at $A(\varphi = 0)$ since at $\varphi = 0$ the two, presumably, largest eigenvalues of the transfer matrix coincide ($\lambda_1 = \lambda_2$) which guarantees, see the original works [20],[21] and [11] for a recent work, the existence of phase transition. Therefore, only the behavior of the solutions of the equation (15) about $\varphi = 0$ is required, as already noticed in [13], remembering of course that (11) must hold. Nevertheless, differently from those authors we do not take the continuum limit. By keeping N finite we will be able to study the large N expansion for the closest zero to the YLES and determine the exponent y_h via comparison with (1).

In order to scan the parameter space of the BEG model for a possible new critical behavior at edge singularities we have found more useful instead of using (15) to take consecutive derivatives of expressions (13), (14) and make some mild hypotheses as shown next.

First of all, from the fact that the YLES is located at $A(\varphi = 0)$ it is natural to assume that the smallest phase among all φ_k , i.e., $\varphi_1 = \pi/N$, corresponds to the closest zero to the YLES, namely $u_1(N) = u(\varphi_1)$. The zero $u(\pi/N)$ is determined from $A(\pi/N)$ via (12). Thus, all we need is a large N expansion for $A(\pi/N)$. Our basic hypothesis is the existence of a region in the parameter space of the BEG model where we are allowed to expand $A(\varphi_1)$ in a Taylor¹ series about $\varphi_1 = 0$:

$$A(\varphi_1) = A(0) + \varphi_1 \left. \frac{dA}{d\varphi} \right|_{\varphi=0} + \frac{\varphi_1^2}{2!} \left. \frac{d^2A}{d\varphi^2} \right|_{\varphi=0} + \dots \quad (16)$$

In order to proceed further we would like to collect information about $d^n A/d\varphi^n$ at $\varphi = 0$. From the first derivatives of (13) and (14) we deduce:

$$[\tilde{x}(b-c) - b\lambda_1] \frac{dA}{d\varphi} = [e^{v\varphi} - 1] \frac{\partial \lambda_1}{\partial \varphi} [(2 + e^{v\varphi})\lambda_1 - a_2] \quad (17)$$

¹Notice that due to the square root in (12), when the YLES is located at $A(0) = -2$ ($u = -1$), the existence of (16) does not always lead to a Taylor expansion for $u_1(N)$, as assumed in [13]

Assuming that $\partial\lambda_1/\partial\varphi$ at $\varphi = 0$ is smooth enough to guarantee that the right handed side of (17) vanishes at $\varphi = 0$ we get:

$$[\tilde{x}(b-c) - b\lambda_1]_{\varphi=0} \frac{dA}{d\varphi}|_{\varphi=0} = 0 \quad (18)$$

Therefore if $\lambda_1 \neq \tilde{x}(b-c)/b$ we derive $(dA/d\varphi)_{\varphi=0} = 0$. Since at $\varphi = 0$ we have double degeneracy $\lambda_1 = \lambda_2$, back in the cubic equation (6) it is possible to show that $\lambda_1 = \lambda_2 = \tilde{x}(b-c)/b$ requires $\tilde{x} = (1-c^2)b^2/|b-c|$. Thus, if $\tilde{x} \neq (1-c^2)b^2/|b-c|$ we have² $(dA/d\varphi)_{\varphi=0} = 0$. Consequently, the second derivatives of (13) and (14) furnish

$$[\tilde{x}(b-c) - b\lambda_1]_{\varphi=0} \frac{d^2A}{d\varphi^2}|_{\varphi=0} = \left[\frac{\lambda_1}{2}(\lambda_1 - \lambda_3) \right]_{\varphi=0} \quad (19)$$

Then, if there is no triple degeneracy $\lambda_1 = \lambda_2 \neq \lambda_3$ and $\tilde{x} \neq (1-c^2)b^2/|b-c|$ we end up with $(dA/d\varphi)_{\varphi=0} = 0$ but $(d^2A/d\varphi^2)_{\varphi=0} \neq 0$. Back in (16) and then in (12) we derive by comparison with (1) the usual result $y_h = 2$ and $\sigma = -1/2$ which generalizes for the BEG model the proof of $\sigma = -1/2$ given in [13] for the Blume-Capel model. On the other hand, if the couplings are such that we have triple degeneracy, using $(dA/d\varphi)_{\varphi=0} = 0 = (d^2A/d\varphi^2)_{\varphi=0}$ it is easy to show that $(d^3A/d\varphi^3)_{\varphi=0} \neq 0$, consequently we have a new critical behavior with $y_h = 3$ and $\sigma = -2/3$ at the edge singularity. For completeness we mention the third case $\tilde{x} = (1-c^2)b^2/|b-c|$ which leads to $(dA/d\varphi)_{\varphi=0} \neq 0$ and $y_h = 1$, consequently $y_h - d = 0$.

Regarding the exponent y_h , the point $u_E = -1$ ($A(0) = -2$), which corresponds to $\beta H_E = \pm i\pi$, is special as we see from (12). Due to the square root in (12) we expect a change from y_h to $y_h/2$ when the edge is located at $u_E = -1$. The values $y_h = 1, 2, 3$ will be replaced by $y_h = 1/2, 1, 3/2$ respectively. Indeed, all such special values for y_h at $u_E = -1$ have been confirmed numerically, though they are not presented here with the exception of $y_h = 3/2$ which appears in table 1 (third line from the bottom) for which $\sigma = -1/3$ instead of $-2/3$. Even in the cases where $y_h = 1, 1/2$ our numerical results based on the FSS relations (1) and (2), seem³ to confirm the relation $\sigma = (d - y_h)/y_h$. It may be appropriate to mention at this point that there exists an analogous special point in the 2D Ising model for which the natural variable is $\tilde{u} = u^2 = \exp -2\beta H$. Namely, the point $\tilde{u} = -1$ ($\beta H_E = \pm i\pi/2$) is also special, see [5], there appears a change from

²It is clear from the cubic equation (6) that in the special case $b = c$ the condition $\lambda_1 \neq \tilde{x}(b-c)/b$ is always satisfied for any finite non vanishing temperature.

³For the cases where $y_h = 1/2$, for odd number of spins, the zeros follow a more complicated pattern (do not lie on a continuous curve apparently) and the numerical uncertainties are larger.

$\sigma = -1/6$ to $-1/9$ at $\tilde{u} = -1$. Henceforth, we concentrate on the triple degeneracy case ($\sigma = -2/3$).

3 Numerical results

In this section we complement our analytic results in favor of a new critical behavior with a numerical study. First of all, we note that $\lambda_1 = \lambda_2 = \lambda_3 = a_2/3$ holds if and only if :

$$a_1 a_2 - 9 a_0^2 = 0 \quad , \quad 3 a_1 - a_2^2 = 0 \quad (20)$$

For the $S = 1$ Ising model ($b = 1 = x$) there is no real temperature, not even in the antiferromagnetic case ($c \geq 1$), at which conditions (20) hold, similarly for the $q = 3$ states Potts model where $b = 1/c^3$ and $\tilde{x} = u/c^3$. However, for the BEG model there are many solutions for the triple degeneracy conditions (20). In what follows we present numerical results for two special cases.

3.1 BEG model with $b = c$ ($K = -J$)

For the BEG model with $b = c$ ($K = -J$) the dependence of the cubic equation on the magnetic field simplifies which allows us to find the YLZ for a larger number of spins. In this case the conditions (20) imply the fine tuning

$$x = x(c) = (1 + c^2) \sqrt{(1 + c^2)/(27(1 - c^2))} \quad (21)$$

and the position of the edge singularity: $A_E = [2(4c^2 - 5)/(1 + c^2)] x(c)$. The singularity is on the left-hand endpoint of an arc on the unit circle (fig. 1a) for $0 \leq c \leq \sqrt{2}/2$ and on \mathbb{R}_- for $\sqrt{2}/2 \leq c \leq 1$, see figures 1a and 1b. We have checked that the YLES on the right-hand endpoint of the arc is of the usual type $\sigma = -1/2$.

In finding the zeros we have started from the expression for the partition function of the BEG model obtained by a diagrammatic expansion similar to what has been done in [19] for the Blume-Capel model. Following the same steps of [19], we first define the generating function of partition functions of the BEG model on non-connected rings and then we take its logarithm which gives rise, as is well known in diagrammatic expansions, to the generating function of only connected diagrams (usual rings). Those steps lead us to $Z_N = -N c^{-N} \{\ln[1 - a_2 g + a_1 g^2 - a_0 g^3]\}_{g^N}$. The notation $\{f(g)\}_{g^N}$ indicates the power g^N in the Taylor expansion of $f(g)$ about $g = 0$. The constant g plays the role of a coupling constant in a diagrammatic expansion *a la* Feynman (perturbation theory). The

above expression for Z_N is equivalent to (5) for arbitrary number of spins. In particular, the reader can easily check it for low number of spins by using the relationships between eigenvalues and coefficients of the cubic equation given in the text between formulae (12) and (13). The new expression turns out to be more efficient than (5) from a computational point of view. In practice, we have used rings with $N_a = 210 + 10(a - 1)$ spins where $1 \leq a \leq 10$. The zeros have been found with the help of Mathematica software. They agree up to the first 30 digits with few cases where they are known exactly as, for instance, $\tilde{x} = c(3 - c^2)^2/2$ and $b = c(3 - c^2)/2$ where, for even number of spins, the Yang-Lee zeros are exactly located at $A_k = -2 - 2i(1 - c^2) \sin(2\pi(1 + 3k)/3N)$, $k = 0, \dots, N - 1$.

According to the discussion at the end of the previous section, we expect $y_h = 3/2$ at $c = \sqrt{2}/2$ where $A_E = -2$, and $y_h = 3$ elsewhere. This is approximately confirmed in table 1. The estimates $y_h^{(1)}$ and $y_h^{(2)}$ refer respectively to di-log fits of (1) and (2) with $L = N$ and $d = 1$. We take the logarithm of the absolute value of the imaginary (real) part of (1) for $0 \leq c \leq \sqrt{2}/2$ ($\sqrt{2}/2 < c \leq 1$) and neglect corrections to scaling in (1) and (2). For both fits we have calculated χ^2 and the deviation from the ideal (± 1) Pearson coefficient, but since they have the same temperature dependence we only display χ^2 in our tables. For $0.1 \leq c \leq 0.5$ the results are quite homogenous but the proximity of the point $\sqrt{2}/2 \approx 0.707$ leads to a crossover behavior at $c = 0.7$ with an increase of 4 orders of magnitude in χ^2 .

Alternatively, from (2) with $d = 1$ and $L = N$, neglecting corrections, we obtain⁴:

$$y_h^{(\rho)}(N_a) = 1 + \left[\ln \frac{N_{a+1}}{N_a} \right]^{-1} \ln \left[\frac{\rho(N_{a+1})}{\rho(N_a)} \right], \quad a = 1, 2, \dots, 9 \quad (22)$$

Some results are shown in table 2 altogether with the $N \rightarrow \infty$ Bulirsch-Stoer (BST) [22, 23] extrapolation. We remark that in the BST approach there is a free parameter w which depends on how we approach the $N \rightarrow \infty$ limit, namely, $y_h(N) = y_h(\infty) + \frac{A_1}{N^w} + \frac{A_2}{N^{2w}} + \dots$. The BST algorithm approximates the original function $y_h(N)$ by a sequence of ratios of polynomials with a faster convergence than the original sequence $y_h(N_a)$. Following [23] we can determine w in a such way that the estimated uncertainty of the extrapolation is minimized. By defining the uncertainty as twice the difference between the two approximants just before the final extrapolated result, see [23], we have tested w in the range $0.5 \leq w \leq 2.5$ and concluded that $w = 1$ is the best choice. All BST results in this work have been calculated at $w = 1$. For $0.1 \leq c \leq 0.6$ the extrapolations are remarkably close to $y_h = 3$. The huge uncertainty at $c = 0.7$ (last row in the third column in table 2) signalizes again the crossover to $y_h = 3/2$. Our numerical results confirm both

⁴A similar formula can be deduced from (1) but it gives results even closer to $y_h = 3$.

finite size scaling relations (1) and (2). See fig.2 for a plot regarding the relation (2).

Before we go to the next case we can, without much numerical effort, check that the triple degeneracy conditions lead in fact to new results. When we choose $b = c$ the equation (15) becomes a cubic equation for $A(\varphi)$. By further fixing $x = x(c)$ according to (21) and $c = 0.4$, for sake of comparison with the zeros in fig.1, we find three solutions $A_i(\varphi)$, $i = 1, 2, 3$ which are still complicated, but expanding about $\varphi = 0$ we derive:

$$A_1(\varphi) = \frac{829}{900} \sqrt{\frac{29}{7}} - \frac{9\sqrt{203}}{400} \varphi^2 + \frac{\sqrt{203}}{1440} \varphi^4 + \mathcal{O}(\varphi^6) \quad (23)$$

$$A_2(\varphi) = -\frac{218}{225} \sqrt{\frac{29}{7}} + \frac{1}{75} \sqrt{\frac{203}{3}} \varphi^3 - \frac{\sqrt{203}}{450} \varphi^4 + \mathcal{O}(\varphi^5) \quad (24)$$

$$A_3(\varphi) = A_2(-\varphi) \quad (25)$$

Now we see that the symmetry $\varphi \rightarrow -\varphi$ of the equation (15) mentioned in [13] does not necessarily lead to even solutions. The operation $\varphi \rightarrow -\varphi$ exchange the second with the third solution. The first solution $A_1(\varphi)$ is the usual Yang-Lee edge singularity and gives $\sigma = -1/2$ while the second one leads to $\sigma = -2/3$. The second solution corresponds to the new edge singularity appearing on the left side of the arcs in fig.1a. The third solution is not a true singularity. We can, even before the expansion about $\varphi = 0$, substitute $A_i(\varphi)$ in the eigenvalue solutions of the cubic equation (6) and check numerically that the magnitude of two eigenvalues degenerates for all $A_i(\varphi)$. However, for $A_3(\varphi)$ such magnitude is smaller than the real (non-degenerate in magnitude) eigenvalue and so it does not satisfy (11).

3.2 Blume-Capel model ($b = 1$)

For the Blume-Capel model $K = 0$ ($b = 1$) the triple degeneracy conditions (20) lead to complicated formulas for both the fine tuning function $\tilde{x} = \tilde{x}(c)$ and the position of the new edge A_E :

$$\tilde{x}(c) = \left\{ 1 - 8c + 10c^2 + 10c^3 - 9c^4 + 3(1 - c^2) \left[(P + Q)^{1/3} + R(P + Q)^{-1/3} \right] \right\}^{1/2} \quad (26)$$

$$A_E = \frac{\tilde{x}(c) [(1 + c)(5 - 15c + 5c^2 + 3c^3) + \tilde{x}^2(c)]}{(1 + c)(1 + c^2) + \tilde{x}^2(c)(2 - 3c)} \quad (27)$$

Where $P = \sqrt{c^3(1 + c - c^2)(1 - 3c - c^2)^2}$, $Q = c^2(5 - 36c + 95c^2 - 90c^3 + 27c^4)$ and $R = c(9c^3 - 20c^2 + 10c - 1)$. In the whole range of temperatures $0 \leq c \leq 1$ the function

$\tilde{x}(c)$ given in (26) runs from +1 to +2, in fact we have approximately⁵ $\tilde{x}(c) \approx 1 + c$. The position of the zeros A_E ranges from -2 to +2 which guarantees, see (9), that the new edge is always on the unit circle on the complex u-plane. However, the finite size numerical calculations reveal that the zeros on the unit circle correspond to a small fraction of whole set of zeros, see fig.3 . Those zeros tend to form a short arc whose right-hand endpoint is a usual YLES with $\sigma = -1/2$ as we have checked. The unusual behavior appears on the left-hand endpoint, whose results are displayed in tables 3 and 4. There is no edge singularity for the other zeros outside the unit circle. For technical numerical reasons we have used $N_a = 96 + (a-1)6$ spins with $1 \leq a \leq 10$ and $0.3 \leq c \leq 0.9$. Although the finite size results move away from $y_h = 3$ as $T \rightarrow 0$ (table 3), the BST extrapolations (table 4) all tend to $y_h = 3$ with increasing uncertainty as $T \rightarrow 0$. In table 4 we only display the limit cases $c = 0.3$ and $c = 0.9$. Since we have noticed that the fraction of zeros on S_1 decreases as $T \rightarrow 0$, our interpretation is that we are closer to a continuum distribution of zeros as the temperature increases and the temperature dependence of $y_h^{(\rho)}(N)$ is a pure finite size artefact. In conclusion, our numerical results are in good agreement with our analytic predictions.

Analogously to what we have done at the end of last subsection, if we now assume $b = 1$, $\tilde{x} = \tilde{x}(c)$ as given in (26) and fix some specific value for the temperature, we show that the expansions of the solutions of the equation (15) around $\varphi = 0$ give both $\sigma = -1/2$ and $\sigma = -2/3$.

4 Conclusion

We have derived for the Blume-Capel and BEG models, analytically and numerically, a new value for the magnetic scaling exponent $y_h = 3$ and edge exponent $\sigma = -2/3$. This is only possible due to a triple degeneracy of the transfer matrix eigenvalues. We have checked that our di-log fits, see e.g. fig.2, are consistent with the finite size scaling relations (1) and (2) which appear around the usual Yang-Lee edge singularity. We stress that the new critical behavior found here is not in conflict with previous numerical and analytic results in the literature. In particular, the proof of $\sigma = -1/2$ given in [12, 9, 11] assumes that in the gap of zeros close to the YLES all eigenvalues are real. In the examples that we have analyzed so far we have verified that this is indeed the case for

⁵Although $\tilde{x}(c) \approx 1 + c$ it is important that $\tilde{x}(c) \neq 1 + c$ since $\tilde{x} = (1 - c^2)b^2/|b - c| = 1 + c$ for $b = 1$ and, as we have discussed after formula (18), at that point we may non longer have $dA/d\varphi = 0$ at $\varphi = 0$. In fact, we have confirmed numerically that $y_h \approx 1$ at this point. It corresponds to a bifurcation point where one curve becomes two disjoint arcs of zeros, see fig.(2c) of [19]

the usual YLES ($\sigma = -1/2$), however only the largest eigenvalue is real in the gap close to the new singularity ($\sigma = -2/3$). Besides, although all eigenvalues are real at vanishing magnetic field, as one can check from (6) at $A = 2$, apparently nothing prevents the two eigenvalues with smallest magnitude of acquiring an imaginary part before reaching the edge singularity as we increase the magnetic field through imaginary values. Consequently, so far we have not been able to prove that the edge singularity closer to \mathbb{R}_+ is always of the usual type ($\sigma = -1/2$), or alternatively, that the triple degeneracy condition could be satisfied also by an edge singularity close to the positive real axis. Concerning the recent proof of $\sigma = -1/2$ given in [13], it supposes that $(d^2u/d\varphi^2)_{\varphi=0} \neq 0$ which is not the case in the examples presented here where $\lambda_1 = \lambda_2 = \lambda_3 \neq \tilde{x}(b-c)/b$.

Finally, it is important to remark that instead of imposing the triple degeneracy conditions (20) and finding rather peculiar fine tuning functions (21) and (26) we could turn the argument around and claim that for some given values of the couplings b and x we can, in many cases, find a specific real temperature c such that conditions (20) are satisfied and the usual result $\sigma = -1/2$ is replaced by $\sigma = -2/3$. Since the number of transfer matrix eigenvalues is infinite for $d > 1$, even for the $S = 1/2$ Ising model, we might speculate that the degeneracy of more than two largest eigenvalues could play a role also in higher dimensional spin models and lead to a change in the exponent σ at specific temperatures in $d > 1$.

5 Acknowledgments

D.D. is partially supported by CNPq and F.L.S. has been supported by CAPES. D.D. has benefited from discussions with A.S. Castro, R.V. de Moraes, A. de Souza Dutra and M. Hott. A discussion with N.A. Alves on the BST extrapolation method is gratefully acknowledged. Special thanks go to Luca B. Dalmazi for some computer runs.

References

- [1] C.N. Yang and T.D. Lee, Phys. Rev. **87** (1952) 404; T.D. Lee and C.N. Yang, Phys. Rev. **87** (1952) 410.
- [2] I. Bena, M. Droz, A. Lipowski, Int. J. Mod. Phys. **B19** 4269 (2005).
- [3] M. Fisher, Phys. Rev. Lett. **40** 1610 (1978).
- [4] J.L. Cardy, Phys. Rev. Lett. **54** 1354 (1985).

- [5] V. Matveev and R. Schrock, Phys. Rev. E **53**, 254 (1996).
- [6] S.-Y. Kim, Phys. Rev. E **74**, 011119 (2006).
- [7] C. Binek in “Ising-type Antiferromagnets”, Springer-Verlag, Berlin (2003), C. Binek, Phys. Rev. Lett. **81** 5644 (1998); .
- [8] S.-Y. Kim, Nucl. Phys. B **705** 504 (2005).
- [9] D.A. Kurze, J. Stat. Phys. **30** 15 (1983).
- [10] Z. Glumac and K. Uzelac, J. Phys. A **27** 7709 (1994).
- [11] X.-Z. Wang and J. S. Kim, Phys. Rev. E **58**, 4174 (1998).
- [12] M. Fisher, Suppl. of the Progr. of Theor. Phys. **69** 14 (1980).
- [13] R.G. Ghulghazaryan, K.G. Sargsyan, and N.S. Ananikian, Phys. Rev. E **76**, 021104 (2007).
- [14] C. Itzykson, R. B. Pearson and J.B. Zuber, Nucl. Phys. B **220** 415 (1983).
- [15] R.J. Creswick, S.-Y. Kim, Phys. Rev. E **56**, 2418 (1997).
- [16] M. Blume, V.J. Emery, and R.B. Griffiths, Phys. Rev. A **4** 1071 (1971).
- [17] T. S. Nielsen and P.C. Hemmer, J. Chem. Phys. **46** 2640 (1967).
- [18] S. Katsura and M. Ohminami, J. Phys. A **5** 95 (1972).
- [19] L.A.F. Almeida and D. Dalmazi, J. Phys. A **38** 6863 (2005).
- [20] E.N. Lassetre and J.P. Howe, J. Chem. Phys. **9**, 747 (1941).
- [21] J. Ashkin and W. E. Lamb, Phys. Rev. **64**, 159 (1943).
- [22] R. Bulirsch and J. Stoer, Numer. Math. **6** 413 (1964).
- [23] M. Henkel and G. Schutz, J. Phys. A **21** 2617 (1988).

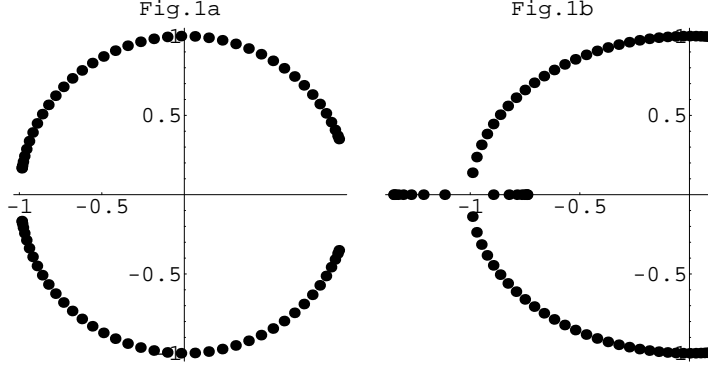


Figure 1: Yang-Lee zeros for the BEG model with $b = c$ on the complex u -plane ($u = \exp^{-\beta H}$) at the triple degeneracy condition, see (21), and temperatures $c = 0.4$ (Fig.1a), $c = 0.9$ (Fig.1b). In both figures we have 100 zeros. The closest zero to the new edge corresponds to $u_1^\pm \approx -0.98602 \pm 0.16660i$ in Fig.1a and $u_1^+ \approx -0.74063$, $u_1^- \approx -1.35021$ in Fig.1b

c	$y_h^{(1)}$	$10^9 \chi_{(1)}^2$	$y_h^{(2)}$	$10^8 \chi_{(2)}^2$
0.1-0.5	2.997	3.5	2.989	4.0
0.6	2.997	3.5	2.987	8.3
0.7	2.880	3.2×10^4	2.094	2.4×10^4
$\sqrt{2}/2$	1.498	0.9	1.494	1.3
0.8	3.000	3.3	2.989	2.3
0.9	2.997	3.5	2.989	3.8

Table 1: Data from di-log fits of formulae (1) and (2) with $L = N$ and $d = 1$ for the $\Delta = -J$ ($b = c$) BEG model with $210 \leq N \leq 300$ spins.

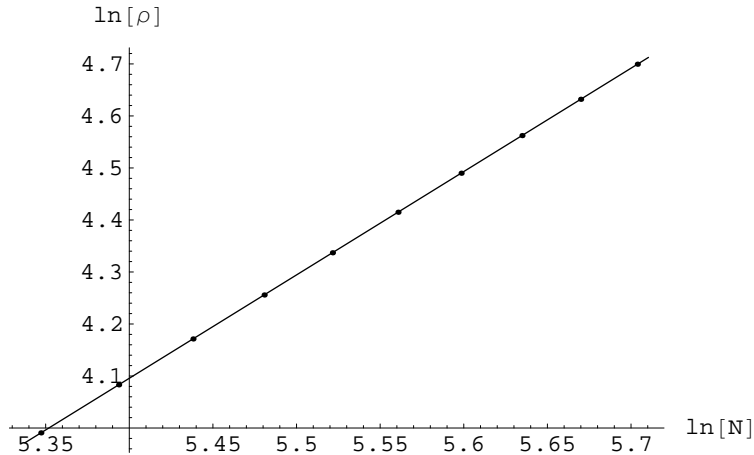


Figure 2: Di-log fit for the density of zeros around the new edge singularity for the $\Delta = -J (b = c)$ BEG model. We have used $210 \leq N \leq 300$ spins at temperature $c = 0.6$. The solid line is $\ln \rho = 1.98724 (\ln N) - 6.63547$.

N_a	$y_h^{(\rho)}(c = 0.6)$	$y_h^{(\rho)}(c = 0.7)$
210	2.98450354337	1.96268002086
220	2.98540244520	1.99853987788
230	2.98619971860	2.03403890400
240	2.98691163425	2.06907936446
250	2.98755121168	2.10357440914
260	2.98812897995	2.13744702199
270	2.98865353760	2.17062929861
280	2.98913197003	2.20306194085
290	2.98957016460	2.23469387995
∞	3.000009(6)	3(8)

Table 2: Finite size results, obtained from (22), for the magnetic scaling exponent y_h for the $(b = c)$ BEG model with $210 \leq N \leq 300$ spins at temperatures $c = 0.6$ and $c = 0.7$.

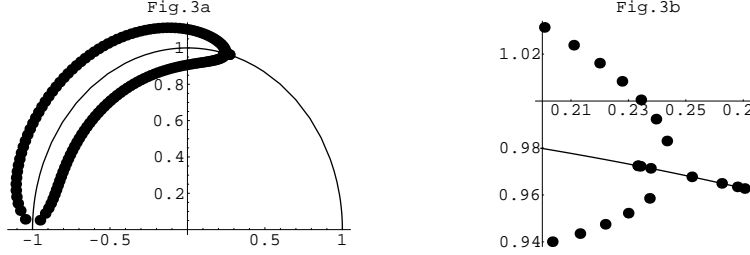


Figure 3: Half ($\text{Im}(u) > 0$) of the Yang-Lee zeros for the Blume-Capel model ($b = 1$) on the complex u -plane ($u = \exp^{-\beta H}$) at the triple degeneracy condition, see (26), temperature $c = 0.5$ and $N = 150$ spins. The solid line in both figures is part of the unit circle. The closest zero to the new edge corresponds to $u_1^+ \approx 0.2332 + 0.9734 i$ as shown in detail in Fig.3b.

c	$y_h^{(1)}$	$10^5 \chi_{(1)}^2$	$y_h^{(2)}$	$10^3 \chi_{(2)}^2$
0.3	3.200	5.03	4.612	3.10
0.4	3.148	2.52	3.795	2.10
0.5	3.119	1.51	3.561	0.72
0.6	3.100	1.00	3.442	0.36
0.7	3.088	0.76	3.370	0.22
0.8	3.078	0.58	3.320	0.15
0.9	3.071	0.48	3.285	0.11

Table 3: Data from di-log fits of formulae (1) and (2), with $L = N$ and $d = 1$, for the Blume-Capel model with $96 \leq N \leq 150$ spins and temperatures $0.3 \leq c \leq 0.9$. We have used $|\Re(u_1^+(N) - u_1(\infty))|$ in the di-log fit of (1).

N_a	$y_h^{(\rho)}(c = 0.3)$	$y_h^{(\rho)}(c = 0.9)$
96	6.65138835174	3.36602639165
102	5.40615603620	3.33723696161
108	4.85302919346	3.31271060187
114	4.52543971437	3.29155556642
120	4.30452579272	3.27311462040
126	4.14377246532	3.25689223008
132	4.02074088023	3.24250742353
138	3.92311802198	3.22966230906
144	3.84352213555	3.21812047991
∞	3.001(1)	3.00000(8)

Table 4: Finite size results, obtained from (22), for the magnetic scaling exponent y_h for the Blume-Capel model ($b = 1$) with $96 \leq N \leq 150$ spins at temperatures $c = 0.3$ and $c = 0.9$.